


# VX-702 Ameliorates the Severity of Sepsis-Associated Acute Kidney Injury by Downregulating Inflammatory Factors in Macrophages

Yue Han\*, Jingyi Wang\*, Jin Zhang\*, Xi Zheng , Yijia Jiang, Wei Liu, Wenxiong Li

Department of Surgical Intensive Care Unit, Beijing Chao-Yang Hospital, Capital Medical University, Beijing, People's Republic of China

\*These authors contributed equally to this work

Correspondence: Wenxiong Li, Department of Surgical Intensive Care Unit, Beijing Chao-Yang Hospital, Capital Medical University, 8 Gongren Tiyuchang Nanlu, Chaoyang District, Beijing, 100020, People's Republic of China, Tel +86 136 0109 7813, Email liwx1126@163.com

**Purpose:** Sepsis-associated acute kidney injury (S-AKI) contributes to high mortality, but it is lack of specific treatments. We aimed to investigate the underlying mechanism of S-AKI and to identify target drugs to alleviate AKI.

**Methods:** We establish a stable mouse model of S-AKI by *Pseudomonas aeruginosa* incision infection. Based on high-throughput sequencing and bioinformatics analysis, we investigated the underlying mechanism and selected the target drug (VX-702) for S-AKI. An in vitro model established by co-cultured of kidney tubular epithelial cell line (TCMK-1) cells with lipopolysaccharide (LPS)-induced leukemic monocyte/macrophage cells (RAW264.7), we explored the effect of VX-702 on S-AKI.

**Results:** The data showed interleukin (IL)-6 and IL-1 $\beta$  were the hub genes, and the mitogen-activated protein kinase (MAPK) signaling pathway was the main pathway involved in S-AKI. Administration of VX-702 by oral gavage decreased the elevated concentrations of IL-6, IL-1 $\beta$ , serum creatinine, and blood urea nitrogen in mice with S-AKI. Moreover, VX-702 reduced the number of apoptotic cells in damaged kidney tissues. Cell viability was decreased, and the number of apoptotic cells was increased in TCMK-1 cells co-cultured with LPS-induced RAW264.7 cells compared to LPS-induced TCMK-1 cells. VX-702 treatment reversed this effect. VX-702 treatment reduced the levels of phosphorylated p38 MAPK and proinflammatory cytokines in RAW264.7 cells and the supernatant. VX-702 could bind IL-6, IL-1 $\beta$  and MAPK, and affect the binding of IL-1 $\beta$  and its receptor, as demonstrated by molecular docking.

**Conclusion:** VX-702 ameliorated S-AKI by inhibiting the release of proinflammatory cytokines from macrophages, indicating its potential as a novel therapeutic for S-AKI treatment.

**Keywords:** sepsis-associated acute kidney injury, VX-702, macrophages, inflammatory factor, MAPK

## Introduction

Sepsis is a complex clinical syndrome that causes tissue destruction and fatal multiple-organ dysfunction.<sup>1</sup> The damage to the kidneys in sepsis cases accounts for approximately 60%.<sup>2</sup> Compared to that patient without acute kidney injury (AKI), patients with sepsis-associated AKI (S-AKI) have a significantly increased risk of mortality, ranging from 24% to 62%.<sup>3</sup> Besides, sepsis survivors tend to have a higher incidence of chronic kidney disease. Unfortunately, no specific drugs or treatments are available for S-AKI patients. Therefore, it is necessary to investigate its underlying mechanisms and explore new therapeutic approaches to improve the outcomes for S-AKI patients.

The pathogenesis of S-AKI is complex and includes inflammation, microvascular dysfunction, and renal tubular damage.<sup>1</sup> Macrophages and renal tubular epithelial cells (TECs) in the kidney play a vital role in the kidney maintenance. The dysfunction or death of these cells is closely involved in S-AKI.<sup>4,5</sup> In particular, macrophages play a central role in

innate immunity during defense against infections.<sup>6,7</sup> Damaged tissues release pathogen-associated molecular patterns (PAMPs) and/or host-derived damage-associated molecular patterns (DAMPs), which are recognized by macrophages through pattern recognition receptors.<sup>8,9</sup> PAMPs and/or DAMPs activate and promote the classically activated macrophages, causing the release of chemokines, reactive oxygen species (ROS) and proinflammatory cytokines (interleukin-1 $\beta$  [IL]-1 $\beta$ , IL-6, tumor necrosis factor- $\alpha$  [TNF- $\alpha$ ]) that damage the kidney tissue.<sup>10,11</sup> Therefore, inhibiting the release of proinflammatory cytokines and reducing the inflammatory response during sepsis may be an effective strategy to prevent and reduce organ injury.

VX-702, was a clinically pre-evaluated and highly selective inhibitors of p38 MAPK, which was shown to regulate production of proinflammatory cytokines in response to lipopolysaccharide (LPS) and in rheumatoid arthritis.<sup>12</sup> It was reported that VX-702 could inhibit osteoclast activation, prevent both the development and progression of collagen-induced arthritis of the disease after the initiation of inflammation.<sup>12</sup> So VX-702 was considered be one of a potential treatment for rheumatoid arthritis and evaluated in phase 2 trial. However, the effect of VX-702 on sepsis and kidney disease is still blank.

The present study aimed to investigate the underlying mechanism of S-AKI using in vivo and in vitro models, and to identify target drugs to alleviate AKI. First, a stable mouse model of S-AKI was established by *Pseudomonas aeruginosa* (*P. aeruginosa*) incision infection. Second, the hub genes involved in S-AKI were identified by high-throughput sequencing and bioinformatics analysis. Then, the related pathways and biological processes were revealed by the Kyoto Encyclopedia of Gene and Genomes (KEGG) and Gene Ontology (GO) enrichment analysis. Third, immunofluorescence and enzyme-linked immunosorbent assay (ELISA) were performed to verify the related pathway, and the target drug (VX-702) of the related pathway was identified. Finally, the curative properties and related pathway-associated regulatory effects of VX-702 were demonstrated in in vivo and in vitro models, offering a potential therapeutic strategy for S-AKI.

## Materials and Methods

### Animals

A total of 90 female adult Balb/c mice (8–10 weeks old) weighing 18–22 g (Vital River Laboratories, Beijing, China) were housed in separate sterile cages and provided free access to water and food. Mice were housed in a room that was specifically pathogen-free, under a 12-h light/dark cycle at 35% humidity and 23.6°C. The experimental procedures were performed in accordance with the principles of the Laboratory Animal Guidelines for Ethical Review of Animal Welfare (GB/T 35892–2018). This study was approved by the Ethics Animal Committee at Capital Medical University on the Use of Animals in Research and Education (Ethics number AEEI-2022–087 and AEEI-2022–090). At the end of the experiments, mice were sacrificed by dislocating the cervical vertebrae under an excessive dose of sodium pentobarbital (100 mg/kg, intraperitoneal injection). Animal death was confirmed by the absence of breathing or heartbeat.

### Bacterial Strain and Suspension Preparation

*Pseudomonas aeruginosa* (*P. aeruginosa*, ATCC 27853, Guangdong Microbial Species Preservation Center, Guangzhou, China) was cultured in Luria-Bertani (LB) medium at 37°C, 200 rpm/min, overnight (Figure 1A). The bacterial suspension was diluted, and 100  $\mu$ L was inoculated onto an LB agar plate and incubated at 37°C overnight (n = 5). Then, the number of colonies on the LB agar plate was counted. The original *P. aeruginosa* concentration was adjusted to 10<sup>10</sup>CFU/mL, 10<sup>9</sup>CFU/mL, 10<sup>8</sup>CFU/mL and 10<sup>7</sup>CFU/mL, based on the number of colonies.<sup>13,14</sup>

### Animal Experiments Design

Mice were anesthetized with 3% isoflurane by inhalation (under 600–800 mL/min oxygen flow rate). S-AKI was induced by incision infection with *P. aeruginosa*.<sup>13–15</sup> A 5 mm median incision was made on the back of the mice to expose the right paravertebral muscle. A 50  $\mu$ L suspension of bacteria was smeared on the right paravertebral muscle. Subsequently, a 5–0 suture was used to seal the incision.

To establish a stable mouse model of S-AKI, 60 mice were divided into six groups (10 mice per group): 10<sup>7</sup> CFU/mL group, 10<sup>8</sup> CFU/mL group, 10<sup>9</sup> CFU/mL group, 10<sup>10</sup> CFU/mL group, sham group and control group. The control group

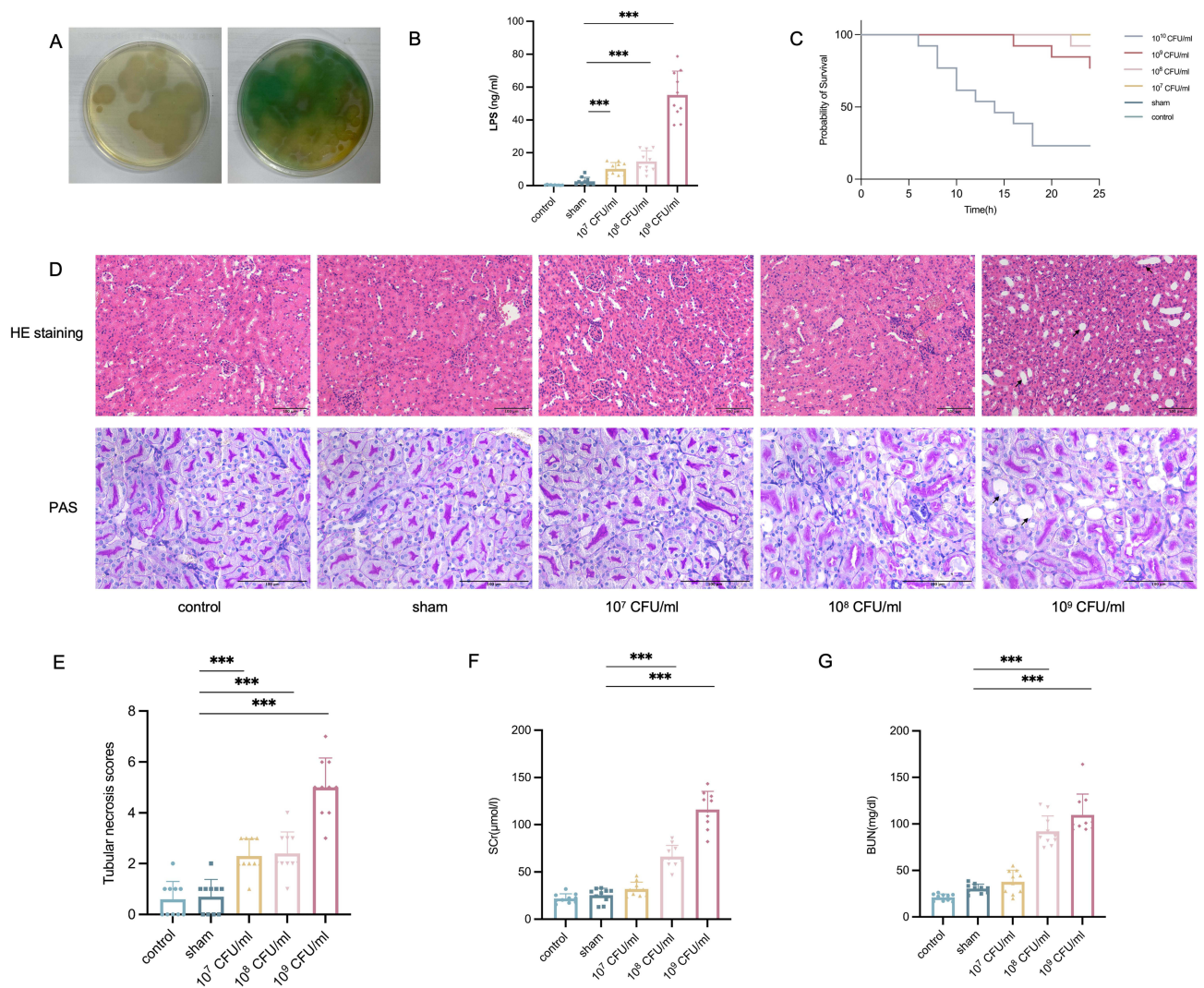


**Figure 1** Establishment of stable S-AKI mice model. **(A)** The LB medium with amplified *P. aeruginosa*. **(B)** The concentrations of LPS in plasma at 24 h after incision infection in different groups (n=10). **(C)** Kaplan-Meier's survival curve of different groups within 24 h after incision infection (n=10). **(D)** Histopathology (HE and PAS staining) of kidney tissues in different groups at 24 h after incision infection. **(E)** The tubular necrosis scores of different groups at 24 h after incision infection. **(F and G)** The concentrations of SCr and BUN at 24 h after incision infection (n=10). Data were expressed as mean  $\pm$  standard deviation. Difference between 10<sup>9</sup> CFU/mL group, 10<sup>8</sup> CFU/mL group, 10<sup>7</sup> CFU/mL group, sham group, and control group was made using unpaired Student's t-test for normally distributed data (n=10). Images,  $\times$  200 and  $\times$  400; original scale bar, 100  $\mu$ m. Arrows indicate the damaged renal tubule. \*\*\*p<0.001.

**Abbreviations:** S-AKI, sepsis-associated acute kidney injury. LB, Luria-Bertani. SCr, serum creatinine. BUN, blood urea nitrogen. HE, hematoxylin and eosin. PAS, Periodic Acid-Schiff.

did not receive any intervention. Mice in the sham group received only back incisions after being anesthetized. Both kidneys were removed 24 h after surgery for high-throughput sequencing and histopathological analysis. Blood samples were collected to determine lipopolysaccharide (LPS), serum creatinine (SCr) and blood urea nitrogen (BUN) levels.

To investigate whether VX-702 affected S-AKI animal model, 30 mice were divided into three groups (10 mice per group): VX-702 group, dimethylsulphoxide (DMSO) group and sham group. The endpoint was 24 h after surgery. Both kidneys and blood samples were collected at 24 h after surgery.

VX-702 was purchased from Beyotime (SD5960, Shanghai, China) and dissolved in DMSO. After performing the back incision, VX-702 was administered at a dose of 50 mg/kg twice daily via oral gavage (o.g.).<sup>16</sup> The DMSO group were administered 5  $\mu$ L DMSO (the maximum concentration of solvent used). Only back incision was performed on the sham group after being anesthetized.

The left side of the mouse kidney tissue was harvested 24 h after surgery for histopathology, immunofluorescence, and TdT-mediated dUTP nick end labeling (TUNEL) assay. Blood samples were collected 24 h after surgery for

examining the levels of inflammatory cytokines, SCr, and BUN. The blood samples were allowed to stand for 30 minutes, then centrifuged at 3000 rpm at 4°C for 10 minutes, and the supernatant was stored at –80°C.

## Cell Culture and Treatment

Mouse kidney tubular epithelial cell line (TCMK-1, ATCC® CCL-139™) was purchased from the American Type Culture Collection (Manassas, VA, United States) and cultured in Dulbecco's modified Eagle medium (DMEM, G4511, Servicebio, Wuhan, China) containing 10% fetal bovine serum (FBS, Gibco, Gaithersburg, MD, USA) at 37°C with 5% CO<sub>2</sub>.

Mouse leukemic monocyte/macrophage cell line (RAW264.7, ATCC®, TIB-71) was purchased from the American Type Culture Collection (Manassas, VA, United States). RAW264.7 cells serve as a useful model to study the mechanisms of inflammation in LPS-induced macrophages. Such LPS-induced RAW264.7 cells reportedly produced proinflammatory factors, including IL-1β, TNF-α and IL-6,<sup>17,18</sup> which may affect S-AKI.

In the present study, RAW264.7 cells were trypsinized and subsequently plated in 24-well plates at a density of 1×10<sup>5</sup> cells/well in 1 mL of DMEM with 10% FBS. TCMK-1 cells were added onto the cell culture inserts (0.4 mm pore diameter) which were placed in the wells with RAW264.7 cells to initiate the in vitro inflammatory reaction by treatment with 1 μM LPS. LPS (L8880, E. coli 055:B5) was purchased from Solarbio (Beijing, China).

To evaluate the inhibition of proinflammatory cytokines and the MAPK protein, 5 μM VX-702 was added to the cells, based on a previous study.<sup>19</sup> Conditioned medium from the cells, co-cultured for 24 h, was collected for cytokine quantification by ELISA. In addition, RAW264.7 and TCMK-1 cells were collected.

## SCr and BUN Assay

SCr and BUN levels were measured using an automatic biochemical analyzer (Chemray 800, Rayto) according to the manufacturer's instructions (Rayto).

## Histopathology

As reported previously, tubular necrosis in the outer medullary region of the kidney was observed at 200x and 400x magnifications.<sup>20–22</sup> Paraformaldehyde solution (10%) was used to fix the kidney tissue. Renal tissue specimens were embedded in paraffin wax and sliced for Periodic Acid-Schiff (PAS) and hematoxylin and eosin (HE) staining. Histopathological analysis was performed by light microscopy. The slides were assessed by a histopathologist who was blinded to the study. All specimens were evaluated for epithelial cell vacuolization, tubular cell flattening, degeneration, tubular dilatation, hyaline cast, and debris materials in the tubular lumen using scores from 1 to 5, wherein a score of zero was assigned to normal tissue without damage.<sup>23</sup>

## High-Throughput Sequencing and Bioinformatics Analysis Methods

High-throughput mRNA sequencing and analysis of kidney tissues were performed by Beijing CapitalBio Technology (Beijing, China). The limma package and DESeq package were applied to study the differential expression of mRNAs between S-AKI kidney samples (n=1) and kidney sham samples (n=1). Genes identified as significantly expressed for each dataset had an absolute log<sub>2</sub> Fold Change value > 1 and a Benjamini-Hochberg adjusted p-value < 0.05.

Protein–protein interaction (PPI) networks were established by the STRING 11.5 database (<https://cn.string-db.org/>).<sup>24,25</sup> The selection confidence score was at least 0.4. The hub genes of the PPI networks were identified using three algorithms: degree, closeness, and betweenness, which were calculated using Cytoscape 3.8.2 software and the cytoNCA application.<sup>26,27</sup>

GO and KEGG analyses were performed by Database for Annotation, Visualization and Integrated Discovery (DAVID) Bioinformatics Resources 6.8 (<https://david.ncifcrf.gov/>).<sup>28,29</sup> For all analyses, p<0.05 and gene enrichment of >2-fold were considered statistically significant.

## Immunofluorescence Analysis

Paraffin-embedded sections of methanol-Carnoy fixed tissue were stained for proinflammatory cytokines (IL-6 and IL-1β). Tissue slices were incubated for 10 minutes with 3% H<sub>2</sub>O<sub>2</sub>, after deparaffinization and hydration. Then, the samples were blocked with 10% bovine serum albumin, and incubated overnight at 4 °C with antibodies (IL-6 [DF6087, Affinity,



Jiangsu, China], IL-1 $\beta$  [26048-1-AP, Proteintech, Wuhan, China], and f4/80 [29414-1-AP, Proteintech, Wuhan, China] at 37°C. Sections were incubated with secondary antibodies in the dark for 1 h and photographed under an epifluorescence microscope.

## Cell Viability Assay

The viability of the TCMK-1 cells was measured using the cell counting kit-8 (CCK-8) assay (Beyotime, Shanghai, China). TCMK-1 cells in the growth phase were seeded in 96-well plates at a density of 5000 cells/well. The cells were incubated at 37°C, then 10  $\mu$ L of CCK-8 reagent was added into each well and the cells were incubated for an additional 2 h. The optical density was measured at 450 nm using a microplate reader (Thermo Fisher Scientific).

## TUNEL Assay

Apoptosis in the kidneys was assessed by the TUNEL assay<sup>30</sup> according to the manufacturer's instruction. TUNEL-positive cells were counted in ten random fields at 400x magnification.<sup>31</sup>

Apoptosis in TECs was assessed using the one-step TUNEL apoptosis assay kit (Beyotime, Shanghai, China) according to the manufacturer's instructions. TUNEL-positive cells were counted in ten random fields at 100x magnification.

## ELISAs

The proinflammatory cytokines (IL-6 and IL-1 $\beta$ ) and LPS in the serum and conditioned medium were assayed using ELISA kits (JL20268 for IL-6, JL18442 for IL-1 $\beta$ , Jnlh, Shanghai, China; SEB526Ge for LPS, Wuhan, China). All procedures were performed according to the manufacturer's instructions.

## Western Blotting

The collected RAW264.7 cells were lysed in RIPA lysis buffer and centrifuged at 12,000 rpm/minute at 4°C for 30 minutes. The supernatant was collected and the protein concentration was determined using the Enhanced BCA Protein Assay kit (Beyotime, Shanghai, China). Proteins (30  $\mu$ g per lane) were separated using a 12% gel by sodium dodecyl sulfate-polyacrylamide gel electrophoresis. The proteins were electrotransferred onto polyvinylidene fluoride (PVDF) membranes (Beyotime, Shanghai, China). After blocking for 30 minutes in Rapid Blocking Solution (Beyotime, Shanghai, China), the PVDF membranes were incubated with primary antibodies, including IL-6 (DF6087, Affinity, Jiangsu, China), IL-1 $\beta$  (RM6784, Biodragon, Suzhou, China), p38 MAPK (AF1111, Beyotime, Shanghai, China), p-p38 MAPK (AM063, Beyotime, Shanghai, China) and  $\beta$ -tubulin (AF2835, Beyotime, Shanghai, China), overnight at 4°C. After washing with tris-buffered saline containing triton X-100 (TBST), the membranes were incubated with the IRDye 680RD secondary antibody (Licor, Hong Kong, China) for 1 h at 26°C and protein bands were detected using the Odyssey Infrared Imaging System.

## Flow Cytometry

Apoptosis was determined using the Annexin V-FITC/propidium iodide (PI) Apoptosis Detection reagent (Servicebio, Wuhan, China). TCMK-1 cells were collected, washed three times, resuspended in binding buffer, and incubated with Annexin V-FITC and PI for 10 min at 26°C in the dark. Apoptotic cells were quantified by flow cytometry (BD Bioscience, USA). Annexin V +/PI- cells indicated early-stage of apoptosis and Annexin V-/PI- cells indicated end-stage of apoptosis. Flow cytometry data were analyzed using the FlowJo V10 software (Treestar Software, USA).

## Scratch Assay

TCMK-1 cells were incubated in a 6-well plate with DMEM (2.5mL/well). A 100  $\mu$ L sterile pipette tip was used to make a scratch on the cell monolayer and wound area was observed under a microscope at 0 h and 24 h after scratching.

## Molecular Docking

Firstly, molecular structure files containing IL-6, IL-1 $\beta$ , MAPK, IL-6R, and IL-1 $\beta$ R were downloaded from the PDB database (<https://www.rcsb.org/>). The PubChem compound database (<https://www.ncbi.nlm.nih.gov/structure/>) provided the structure of VX-702.

Protein-ligand structures and water molecules were eliminated using the PyMOL software (<https://pymol.org/2/>). The binding energy and molecular docking were performed using the Autodock 4.2 software (<https://autodock.scripps.edu/downloads>). The hydrogen bond and binding site between the receptor and the ligand were displayed using the PyMOL program.

## Statistical Analysis

SPSS 25.0 software (SPSS Inc., Chicago, IL, USA) was used to analyze the data. The data were presented as the means  $\pm$  SDs. Student's *t*-test was performed for comparisons between the two groups, and comparisons between more than two groups were performed using one-way analysis of variance. Enumeration data were represented by the occurrence rate and compared using the Chi-square test or Fisher's exact test. Statistical significance was set at  $p < 0.05$ .

## Results

### Establishment of a Stable Mouse Model of S-AKI by *P. aeruginosa* Incision Infection

Compared to mice in the control and sham groups, those daubed with incisions using *P. aeruginosa* showed lethargy, body crouching, sluggish responsiveness to the outside environment, inactive eating and drinking, and an increased respiratory rate. The concentrations of LPS in plasma were increased in the  $10^7$ ,  $10^8$ , and  $10^9$  CFU/mL groups compared to the control and sham groups (Figure 1B). The 24 h mortality rate was 8% in the  $10^8$  CFU/mL group, 23% in the  $10^9$  CFU/mL group, 77% in the  $10^{10}$  CFU/mL group, and 0% in the other groups (Figure 1C). HE and PAS staining showed no obvious abnormal changes in the glomeruli and renal tubules in the control and sham groups. Mice in the  $10^9$  CFU/mL group showed apparent infiltration of inflammatory cells, swelling of TECs, the disappearance of brush edges, expansion of the lumen, disordered and lost arrangement of the renal tubular structure, and stenosis of the interstitial part (Figure 1D). The acute tubular necrosis scores were increased in mice in the  $10^7$ ,  $10^8$ , and  $10^9$  CFU/mL groups compared to the control and sham groups (Figure 1E). The concentrations of SCr and BUN were higher in the  $10^9$  CFU/mL group than in the other groups, and the difference was statistically significant (Figure 1F and G). Based on the mortality rate, analysis of renal histopathological sections, SCr and BUN levels,  $10^9$  CFU/mL *P. aeruginosa* were daubed in the incision to establish a mouse model of S-AKI.

### Alternation in the mRNA Expression Profile After *P. Aeruginosa* Infection in Mice with S-AKI

To further elucidate the molecular mechanisms of *P. aeruginosa*-infected mice with S-AKI, high-throughput sequencing was performed using kidney tissues of mice in the S-AKI and sham groups. Genes identified as significantly expressed for each dataset had an absolute log<sub>2</sub> Fold Change value  $> 1$  and a Benjamini-Hochberg adjusted  $p$ -value  $< 0.05$ . As illustrated in Figure 2A, 475 genes were upregulated and 433 genes were downregulated in S-AKI kidney tissues. Additionally, the differential gene expression was evident in the volcano plot (Figure 2B). The STRING 12.0 database was used to construct the PPI network, which included 783 differentially expressed genes (DEGs) (Figure 2C). After analyzing the PPI network using Cytoscape 3.9.0 software, the top five DEGs were confirmed using three different calculation methods (Figure 2D). The intersection of the different top three DEGs was IL6 and IL1 $\beta$  (Figure 2E).

The expression of hub genes was validated by immunofluorescence and ELISA. The kidneys of mice with S-AKI had increased levels of IL-6 and IL-1 $\beta$  compared to mice in the sham group (Figure 3A and B). The concentrations of IL-6 and IL-1 $\beta$  in the serum were significantly higher in mice with S-AKI compared to mice in the sham group (Figure 3E and F).

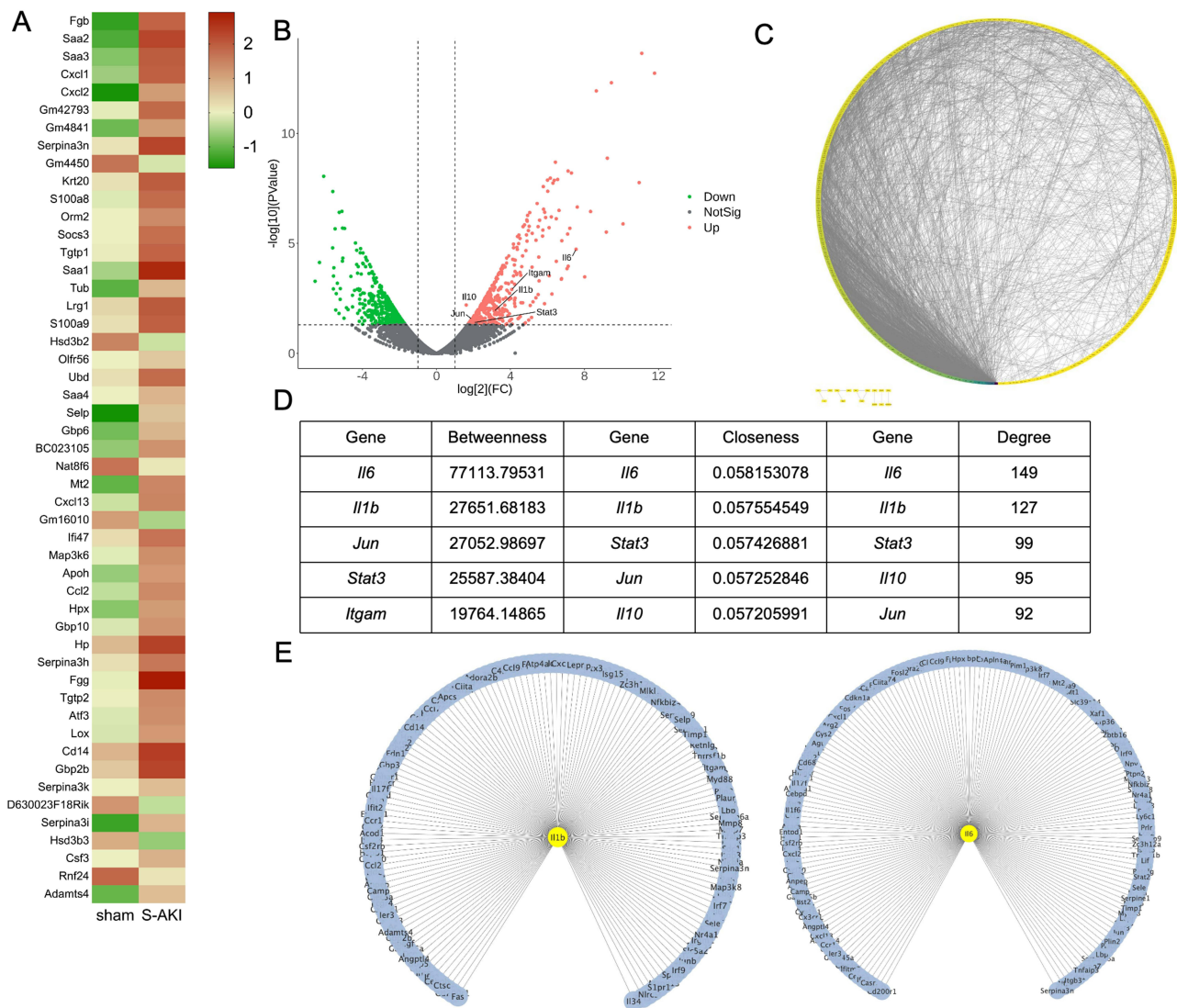


**Figure 2** RNA sequencing results indicate the hub genes. **(A)** Heat map shown the top 50 DEGs of S-AKI group (n=1) vs sham group (n=1). **(B)** Volcano plot of the upregulated genes, downregulated genes and non-regulated genes. Red points represented the 475 upregulated genes, green points represented the 433 downregulated genes. The top 5 DEGs were labeled in the volcano plot. **(C)** PPI network of the DEGs. Cytoscape software was used to calculate the degree value of genes. Low degree value was shown in yellow and high degree value was shown in blue. **(D)** The top 5 DEGs of three algorithms. The intersection of the different top 3 DEGs were IL-6 and IL-1 $\beta$  as the hub genes. **(E)** The hub genes and related direct regulation genes.

**Abbreviations:** DEGs, differential expression genes. S-AKI, sepsis-associated acute kidney injury. PPI, protein-protein interaction. IL, interleukin.

## TNF Signaling and the MAPK Signaling Pathways Were the Main Pathways That Were Enriched

We further examined GO and KEGG analyses using the DAVID database. In molecular function, 230 DEGs were enriched in protein binding, 37 DEGs were enriched in transmembrane transporter activity and 108 DEGs were enriched in identical protein binding (Figure 4A). Moreover, 65 DEGs were enriched in the immune system process, 57 DEGs were enriched in the innate immune response, and 49 DEGs were enriched in the inflammatory response, which was the main biological process (Figure 4B). In the cellular component, 158 DEGs were enriched in the extracellular space, 303 DEGs were enriched in the membrane, and 146 DEGs were enriched in the extracellular region (Figure 4C). The top ten KEGG pathways are summarized in Figure 4D. Significantly enriched KEGG pathways included the TNF and MAPK signaling pathways (Figure 4E).

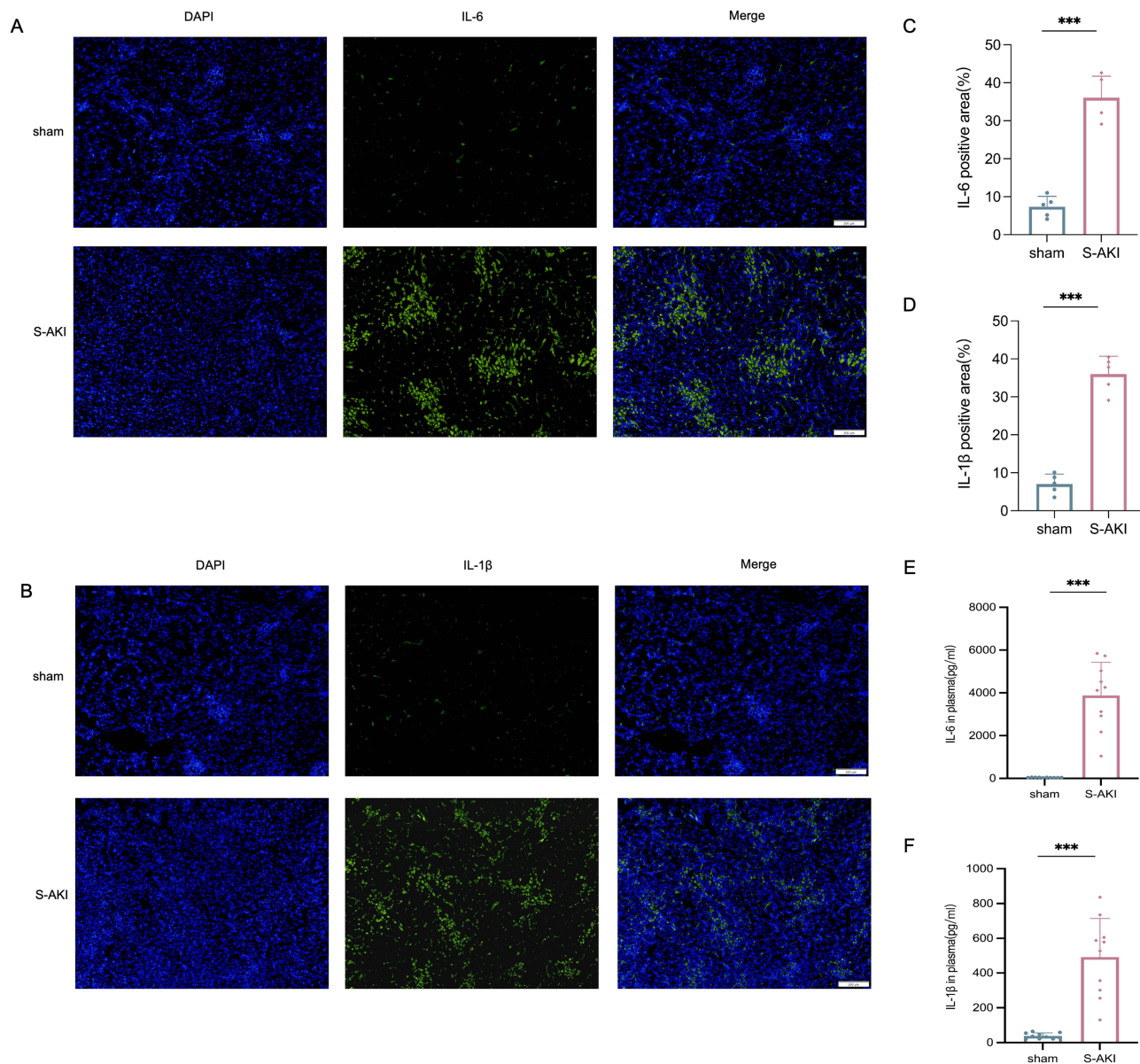


**Figure 3** The hub genes expression in S-AKI. **(A and B)** The immunofluorescence of hub genes of S-AKI group vs sham group. Images,  $\times 100$ ; original scale bar, 200  $\mu\text{m}$ . **(C and D)** Quantification was represented in panel (n=10). **(E and F)** The concentrations of IL-6 and IL-1 $\beta$  in serum (n=10). Data were expressed as mean  $\pm$  standard deviation. Difference between S-AKI group and sham group was made using unpaired Student's t-test for normally distributed data. \*\*\* $p < 0.001$ . **Abbreviations:** S-AKI, sepsis-associated acute kidney injury. IL, interleukin.

## Alleviated the Severity of S-AKI

VX-702, a p38 MAPK inhibitor, is potent and effective against LPS-induced IL-6, IL-1 $\beta$  and TNF- $\alpha$  production as reported previously. VX-702 decreased the mortality of mice with S-AKI (Figure 5A). The concentrations of SCr and BUN were significantly lower in mice treated with VX-702 than in those treated with DMSO (Figure 5B and C). The acute tubular necrosis scores were significantly lower in the VX-702 group than in the DMSO group (Figure 5F). Mice treated with VX-702 showed fewer pathological changes as observed in renal histopathological sections, such as exfoliated epithelial cells, interstitial inflammatory cells, and fragments in the renal tubular lumen (Figure 5D). To assess whether VX-702 treatment affected the extent of apoptosis in the kidney, we performed the TUNEL assay to detect apoptotic cells in the kidney tissues. The number of apoptotic cells increased in mice after incision infection (Figure 5E and G). Mice in the VX-702-treated group had fewer TUNEL-positive cells than those in the DMSO-treated



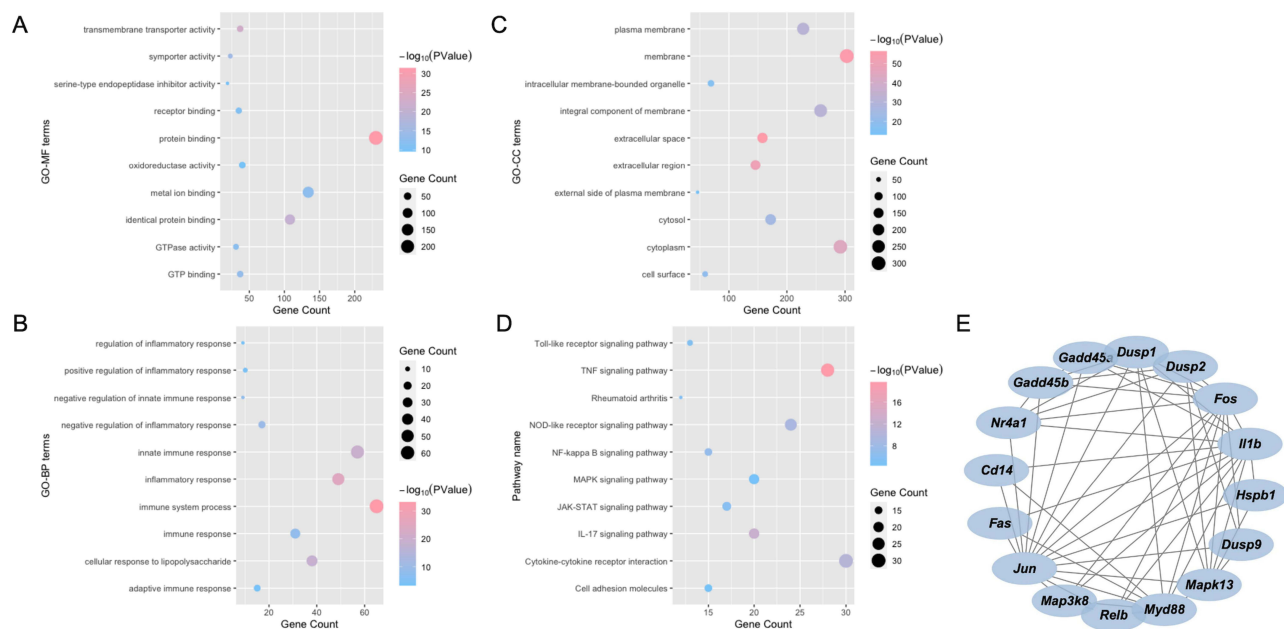


**Figure 4** GO and KEGG enrichment results of 903 DEGs. (A) The molecular function enrichment in GO analysis results. (B) The biological process in GO analysis. (C) The cellular component in GO analysis. (D) The KEGG pathways analysis results. Significantly enriched KEGG pathways included the TNF signaling pathway and the MAPK signaling pathway. (E) The PPI network of MAPK signaling pathway.

**Abbreviations:** GO, gene ontology. KEGG, Kyoto Encyclopedia of Genes and Genomes. DEGs, differential expression genes. MAPK, mitogen-activated protein kinase. TNF, tumor necrosis factor.

group. We evaluated the effects of VX-702 on infection-induced inflammation through immunofluorescence. The concentrations of IL-6 and IL-1 $\beta$  in the serum were detected by ELISA. The numbers of F4/80<sup>+</sup> macrophages were increased in S-AKI group, whereas the number of F4/80<sup>+</sup> macrophages was lower in the VX-702 group than in the S-AKI group (Figure 5H and I). VX-702 treatment decreased IL-6 and IL-1 $\beta$  expression in the kidney tissues of mice with S-AKI and the difference was statistically significant (Figure 5H and I). The location of proinflammatory cytokines (IL-6 and IL-1 $\beta$ ) appeared to colocalize with F4/80<sup>+</sup> macrophages. In addition, VX-702 decreased the concentration of IL-6 and IL-1 $\beta$  in the serum (Figure 5J and K). These results indicated that VX-702 alleviated the severity of S-AKI by reducing the inflammation.

## Establishment of the LPS-Induced RAW264.7 Cell Model and Co-Culture with TCMK-1 Cells

To further investigate the mechanism by which VX-702 mitigates the severity of S-AKI, we treated TCMK-1 cells with LPS to establish an LPS-induced cell model of S-AKI. Cell viability was determined using the CCK-8 assay. Cell scratch assay was performed to evaluate the cell proliferation. Flow cytometry and TUNEL assay were performed to evaluate cell apoptosis. Based on a previous study, we tried different concentration of LPS (from 10 $\mu$ M to 1mM, 3 samples for each concentration) to treat TCMK-1 cells.<sup>32–35</sup> However, there was no significant difference in cell viability, cell proliferation and apoptosis between the LPS-induced TCMK-1 cells and the control group (Figure 6 and Figure S1). Therefore, we established a cell model wherein LPS-induced RAW264.7 cells were co-cultured with TCMK-1 cells. As shown in Figure 6, compared to the control group, the LPS-induced TCMK-1 group and the M $\phi$ +TCM group, the number of apoptotic cells were increased in TCMK-1 cells co-cultured with RAW264.7 cells after LPS treatment, which was demonstrated by TUNEL assay and the flow cytometry (Figure 6B, C, E and F). Moreover, the results of the CCK-8 and cell scratch assays confirmed that co-culture resulted in significant differences in cell viability and cell proliferation (Figure 6A, D and G).

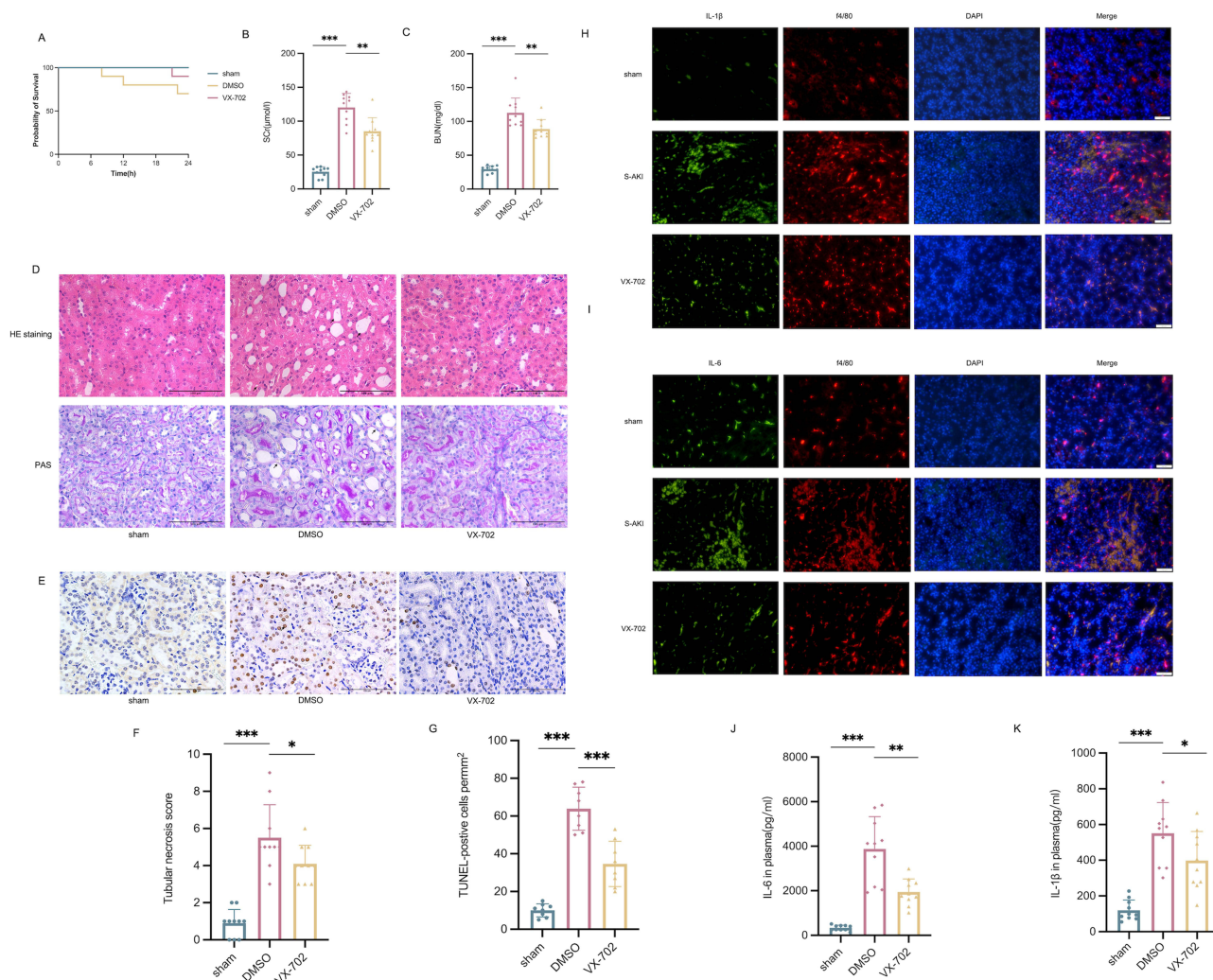


**Figure 5** VX-702 alleviated the severity of S-AKI. **(A)** Kaplan-Meier's survival curve of different groups within 24 h after incision infection. **(B and C)** The concentrations of SCr and BUN at 24 h after incision infection (n=10). **(D)** Histopathology (HE and PAS staining) of kidney tissues at 24 h after incision infection. Images,  $\times 400$ . **(E)** The TUNEL assay of kidney tissues at 24 h after incision infection. Images,  $\times 400$ . **(F and G)** Quantification was represented in panel. **(H and I)** The immunofluorescence of IL-1 $\beta$  and IL-6 in kidney tissues at 24 h after incision infection. Images,  $\times 200$ . **(J and K)** The concentrations of IL-6 and IL-1 $\beta$  in serum (n=10). Original scale bar, 100  $\mu\text{m}$ . Data are expressed as mean  $\pm$  standard deviation. The difference between sham group, DMSO group and VX-702 group was made using unpaired Student's t-test for normally distributed data. Arrows indicate the damaged renal tubule. \* $p < 0.05$  \*\* $p < 0.01$  \*\*\* $p < 0.001$ .

**Abbreviations:** S-AKI, sepsis-associated acute kidney injury. IL, interleukin. SCr, serum creatinine. BUN, blood urea nitrogen. HE, hematoxylin and eosin. PAS, Periodic Acid-Schiff.

## Inhibited Apoptosis and Enhanced the Viability of TCMK-1 Cells

VX-702 treatment significantly enhanced wound closure compared to DMSO treatment (Figure 6). As shown by TUNEL assay and the flow cytometry, the number of positive TCMK-1 cells after VX-702 treatment was significantly lower than that after DMSO treatment (Figure 6). These results indicated that VX-702 inhibited apoptosis and enhanced cell proliferation. Moreover, the results of CCK-8 assay confirmed that VX-702 increased cell viability compared to the DMSO group (Figure 6).

## Treatment with VX-702 Inhibited p38 MAPK Phosphorylation and Mitigated the Expression of Proinflammatory Cytokines in RAW264.7 Cells

To provide evidence that macrophage-mediated release of proinflammatory cytokines is responsible for VX-702 inhibiting TCMK-1 cell apoptosis and alleviating the severity of S-AKI, the levels of proinflammatory cytokines in the LPS-induced RAW264.7 cell supernatant and the co-culture supernatant were examined. The secretion of proinflammatory

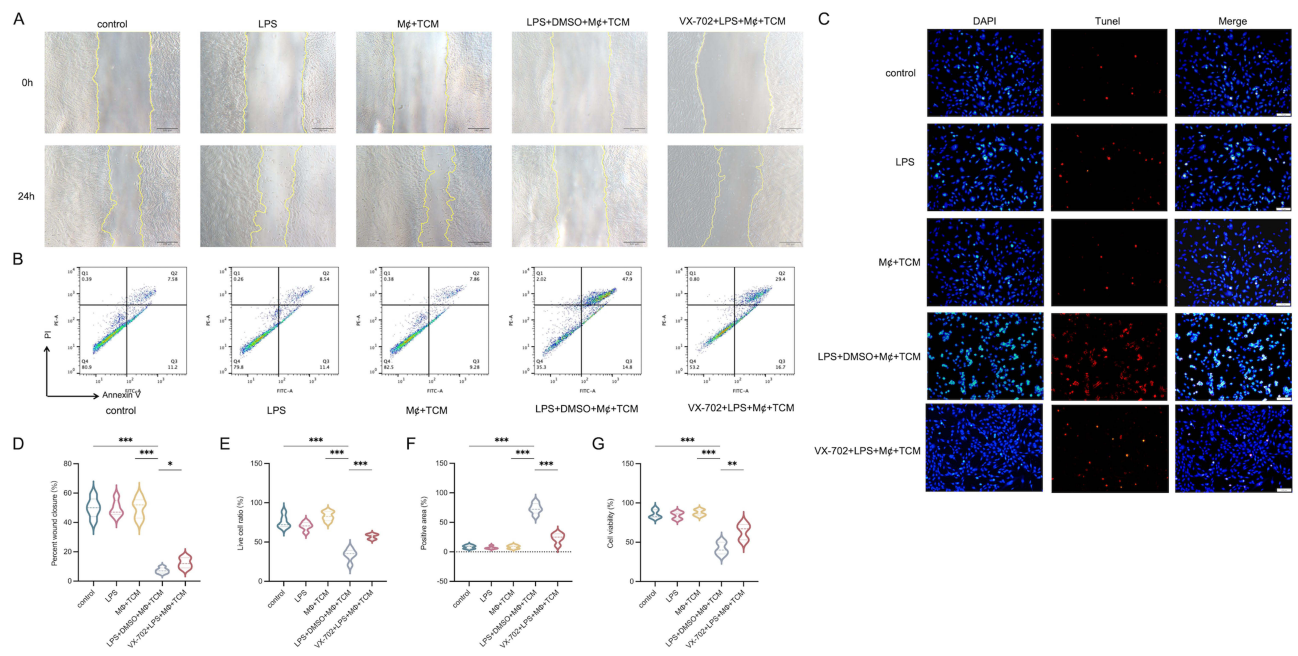


**Figure 6** Establishment of the S-AKI in vitro model and the role of VX-702 on TCMK-1 viability and apoptosis. **(A)** Cell scratch assay results. Images  $\times 40$ ; original scale bar, 100  $\mu\text{m}$ . **(B)** The results of Annexin VI and PI assay. **(C)** The TUNEL images of the apoptosis cells (red fluorescence). images,  $\times 200$ ; original scale bar, 100  $\mu\text{m}$ . **(D, E and F)** Quantification was represented in panel. **(G)** The results of CCK-8 assay results. Data were expressed as mean  $\pm$  standard deviation. Difference was made using unpaired Student's *t*-test for normally distributed data. \* $p < 0.05$  \*\* $p < 0.01$  \*\*\* $p < 0.001$ .

**Abbreviations:** S-AKI, sepsis-associated acute kidney injury. TCMK-1, mouse kidney tubular epithelial cell line. PI, propidium iodide. TUNEL, TdT-mediated dUTP nick end labeling. CCK-8, cell counting kit-8.

cytokines IL-6 and IL-1 $\beta$  in the supernatant was subsequently detected by ELISA. The concentrations of these proinflammatory cytokines were significantly lower in the VX-702-treated group than in the DMSO-treated group both in the LPS-induced RAW264.7 cell supernatant (Figure S2) and co-culture supernatant (Figure 7A and B). Furthermore, we investigated the expression of p38 MAPK protein in LPS-induced RAW264.7 cells after VX-702 treatment. Western blot analysis revealed that the expression levels of IL-6, pro IL-1 $\beta$ , cleaved IL-1 $\beta$  and p-p38 MAPK were decreased in the VX-702 group, as compared to the DMSO group (Figure 7C-H). These results suggested that VX-702 inhibited p38 MAPK phosphorylation and reduced the release of proinflammatory cytokines in LPS-induced RAW264.7 cells.

## VX-702 Could Affect the Binding of IL-1 $\beta$ and IL-6 with Their Receptors

Molecular docking was performed to predict the binding energy of VX-702 with IL-1 $\beta$ , IL-6 and MAPK. The binding energy of VX-702 with IL-6, IL-1 $\beta$ , and MAPK were all below zero, which demonstrated that VX-702 could directly bind with IL-6 and IL-1 $\beta$  besides MAPK (Figure 8). Then, we simulated the effect upon VX-702 binding with the cytokines (IL-6 and IL-1 $\beta$ ) and their receptors. It showed that VX-702 increased the binding energy of IL-1 $\beta$  mildly.

## Discussion

S-AKI is strongly associated with a higher risk of in-hospital death or a prolonged hospital stay.<sup>36</sup> However, the exact mechanism of sepsis remains unclear and there is still a lack of therapeutic interventions. In our study, we demonstrated the protective effects of VX-702 in S-AKI, providing new evidence regarding its potential as a therapeutic.

In previous studies, the cecum ligation and puncture model and the LPS-injected model are the most common models for the investigation of S-AKI.<sup>37</sup> Nevertheless, due to the lack of a standard for length ligation, the different length of the cecum leads to significant variations in the corresponding mortality rates, making it challenging to create a stable model of S-AKI.<sup>38</sup> LPS dosage significantly affects the stability of S-AKI model. Low-dose LPS reduced kidney damage and promoted self-healing. High-dose LPS usually decreased cardiac output, normalized, or increased vascular resistance,

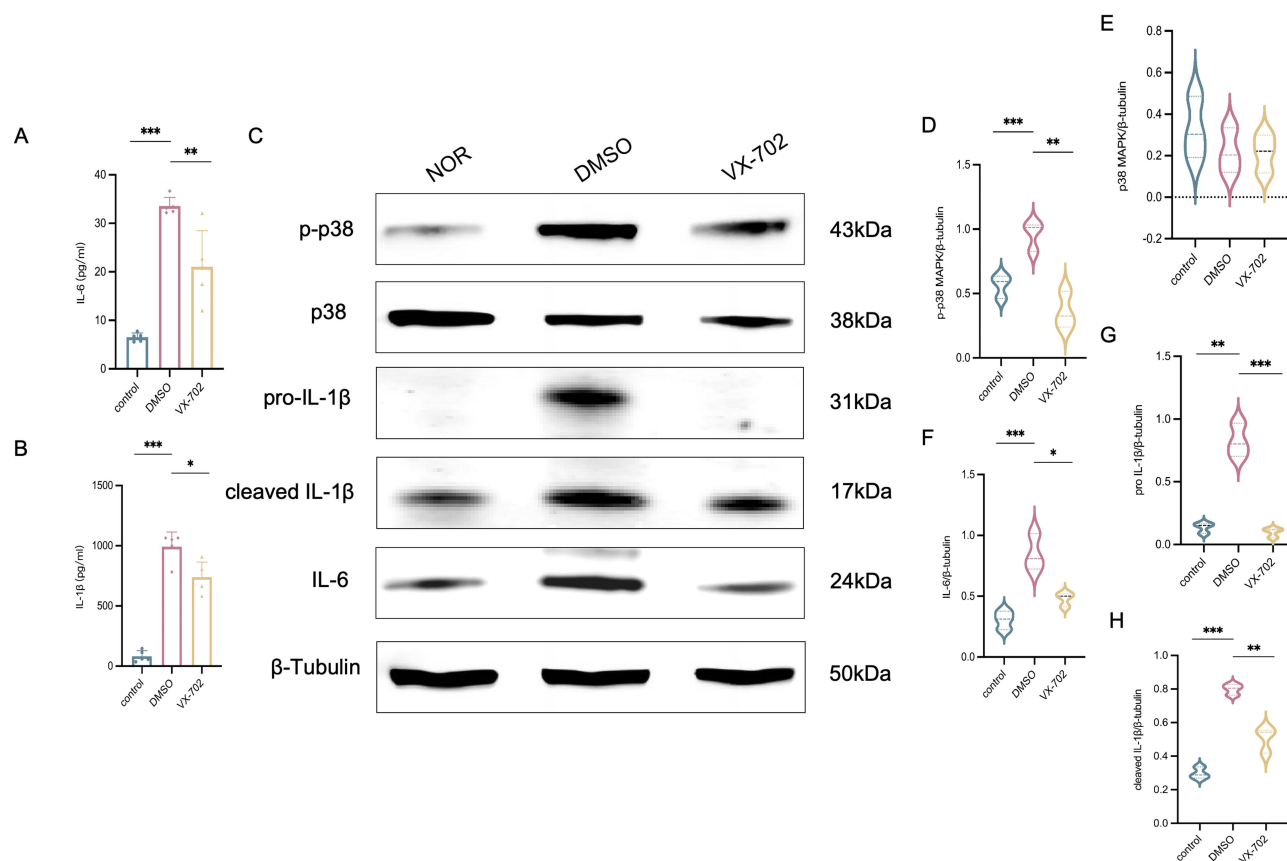


**Figure 7** Effect of VX-702 on proinflammatory cytokines production and MAPK activation in LPS-induced RAW264.7. **(A and B)** The secretions of proinflammatory cytokines IL-6 and IL-1 $\beta$  in the supernatant. **(C)** The results of Western blot analysis in RAW264.7 with indicated antibodies against IL-6, pro IL-1 $\beta$ , cleaved IL-1 $\beta$ , p38 MAPK and p-p38 MAPK. **(D-H)** Expressions of IL-6, pro IL-1 $\beta$ , cleaved IL-1 $\beta$ , p38 MAPK and p-p38 MAPK were quantified by densitometry and normalized with  $\beta$ -tubulin. Data were expressed as mean  $\pm$  standard deviation. Difference was made using unpaired Student's t-test for normally distributed data. \* $p < 0.05$  \*\* $p < 0.01$  \*\*\* $p < 0.001$ .

**Abbreviations:** IL, interleukin. p-p38, phosphorylation of p38. MAPK, mitogen-activated protein kinase. RAW264.7, mouse leukemic monocyte/macrophage cell line.

which is inconsistent with the early changes such as high output and low resistance in sepsis, resulting in high mortality rate. LPS injections caused a rapid short-term rise in cytokine levels, which was contradictory with the limited, low and long-lasting levels as detected in patients with sepsis.<sup>39</sup> Therefore, we established a stable mouse model of S-AKI by incision infection with *P. aeruginosa* in our previous study.<sup>14</sup> This incision infection model was complicated with secondary bloodstream infection, resulting in sepsis, which demonstrated by LPS levels in serum. It was reported that serum LPS is effective in the early detection of bloodstream infections caused by Gram-negative bacteria.<sup>40</sup> After daubing with different bacterial concentrations, serum LPS levels were increased in all infected groups ( $10^7$  CFU/mL,  $10^8$  CFU/mL and  $10^9$  CFU/mL), compared with control and sham groups. LPS as a component of Gram-negative bacteria's cell wall can activate inflammatory cells and factors in tissue, resulting in severe pathophysiological symptoms like sepsis, or multiple organ failure. Considering the LPS, SCr, BUN levels, and mortality, we used  $10^9$  CFU/mL *P. aeruginosa* to establish a satisfactory and stable S-AKI model.

HE and PAS staining revealed TECs edema, interstitial thickening, luminal dilation and inflammatory cell infiltration occurred after incision infection. A dysregulated inflammatory response may cause further injury, resulting in maladaptive repair.<sup>37</sup> To confirm this, the kidney samples were subjected to high-throughput sequencing. The results showed that the hub genes were IL-6 and IL-1 $\beta$  based on three different algorithm analyses, verified by immunofluorescence and ELISA. Excessive production of proinflammatory cytokines is considered an important pathogenic factor in S-AKI. During sepsis, DAMPs and PAMPs are released into intravascular compartments. When exposed to DAMPs and PAMPs filtered through the glomerulus or neighboring peritubular capillaries, proximal TECs show increased production of ROS,



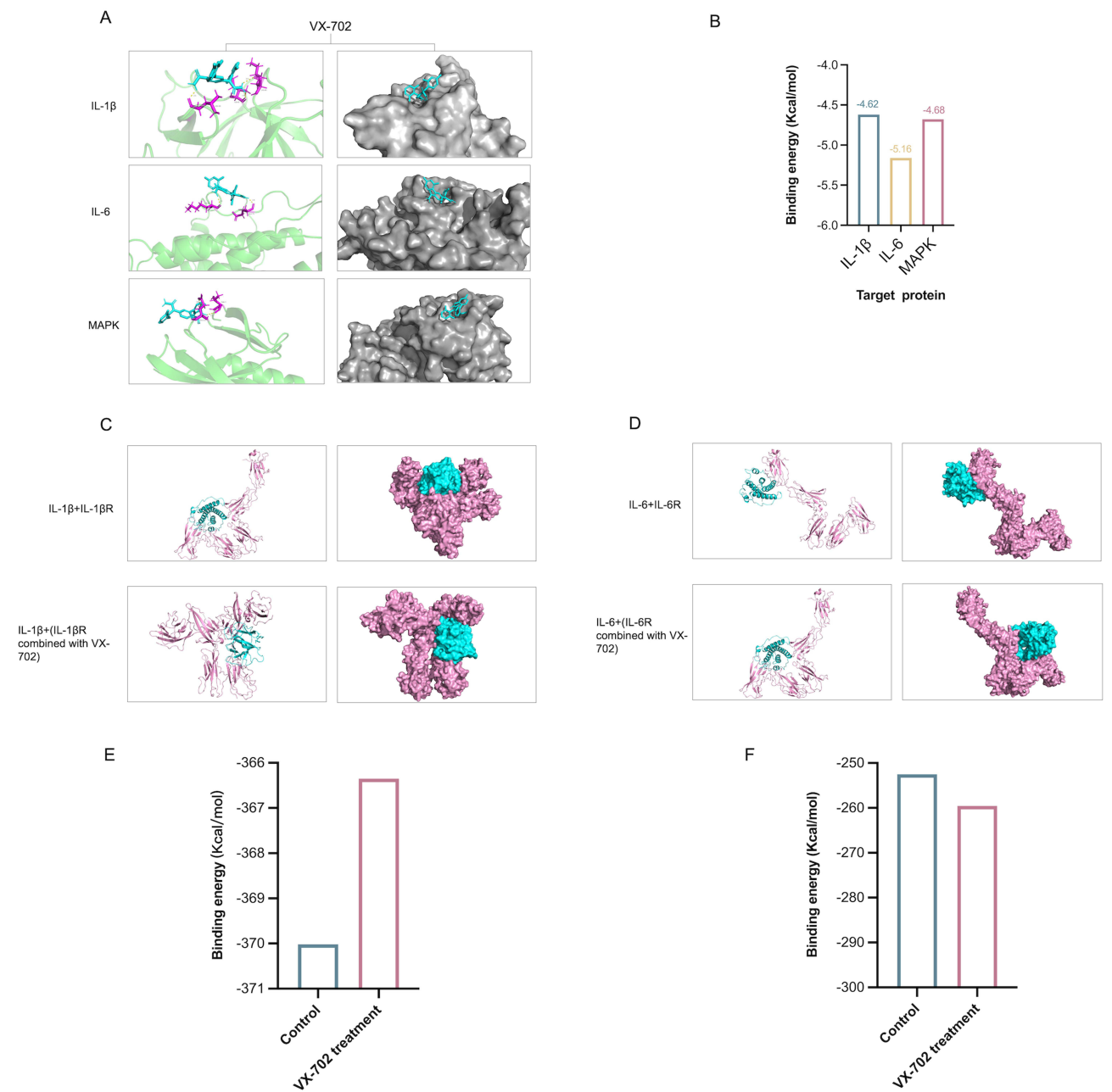


**Figure 8** Molecular docking results of VX-702. (A) Molecular docking results showed the binding site of VX-702 with the target genes. (B) The results of the binding energy of molecular docking. VX-702 could directly bind with IL-6, IL-1 $\beta$  and MAPK. (C) Molecular docking results showed the binding site of IL-1 $\beta$  and IL-1 $\beta$ R with or without VX-702 treatment. (D) Molecular docking results showed the binding site of IL-6 and IL-6R with or without VX-702 treatment. (E and F) The results of the binding energy (E for IL-1 $\beta$ , F for IL-6) of molecular docking.

**Abbreviations:** IL, interleukin. IL-6R, IL-6 receptor. IL-1 $\beta$ R, IL-1 $\beta$  receptor. MAPK, mitogen-activated protein kinase.

oxidative stress, and mitochondrial injury, all of which exacerbate the TECs injury.<sup>41–43</sup> Therefore, the inflammatory cascade and proinflammatory cytokine release may play a vital role in S-AKI.

The DAVID was used to perform the GO and KEGG analyses of the 908 DEGs. According to KEGG analyses, the MAPK signaling pathway was the main enriched pathway in S-AKI patients. MAPKs are classic inflammation-related signals that include extracellular signal-related kinase, p38, and c-Jun NH2-terminal kinase.<sup>44</sup> After recognizing an endotoxin, p38 MAPK, an intracellular signaling protein, is activated.<sup>45</sup> Once activated, the downstream substrates of p-p38 MAPK initiate a signaling cascade that regulates the synthesis of various inflammatory mediators including cytokines (eg, IL-1 $\beta$ , IL-6 and TNF- $\alpha$ ).<sup>46,47</sup> In LPS-induced model of acute lung injury, p38 MAPK was an important

mediator of the inflammatory response.<sup>48</sup> Bode JG found that cytokines, such as TNF- $\alpha$ , IL-1 $\beta$ , and IL-6 released mainly via the p38 MAPK signaling pathway, played a key role in ARDS.<sup>49</sup> Specific and selective p38 MAPK inhibitors block the production of IL-1 $\beta$  and IL-6 in vitro and in vivo.<sup>19,50</sup> Based on recent reports and our results, we hypothesized that a p38 MAPK inhibitor might reduce the damage caused by S-AKI by decreasing the release of inflammatory cytokines.

VX-702 is a highly selective inhibitor of the  $\alpha$  isoform of p38 MAPK that binds to its ATP pocket and inhibits the kinase competitively. In two, double-blind, placebo-controlled studies, VX-702 showed clinical efficacy and suppressed inflammatory biomarkers in patients with active, moderate to severe rheumatoid arthritis.<sup>12</sup> In these studies, VX-702 provided a rapid reduction in the number of tender and swollen joints as early as 2 weeks following initiation of therapy. There was a rapid reduction in the levels of biomarkers of inflammation (IL-1 $\beta$ , IL-6, and C-reactive protein). Previous studies have demonstrated the efficiency of VX-702 in reducing proinflammatory cytokines via the p38 MAPK signaling pathway, implying its potential to alleviate S-AKI. In our study, we evaluated its curative effects in a model of incision infection-induced S-AKI.

Based on clinical view and operational feasibility, VX-702 was administered by oral gavage after the mice underwent back incision. Consistent with previous studies,<sup>19</sup> we also proved that VX-702 reduced the concentration of proinflammatory cytokines (IL-1 $\beta$  and IL-6) in the kidney. Excessive production of proinflammatory cytokines is considered an important pathogenic factor in S-AKI.<sup>51</sup> Our results indicated that VX-702, which exhibits anti-inflammatory activity could be beneficial for S-AKI. We found that VX-702 treatment decreased the mortality and reduced the damage by lowering SCr and BUN levels in mice with S-AKI. Mice treated with VX-702 showed fewer pathological changes in renal histopathological sections, such as exfoliated epithelial cells, interstitial inflammatory cells, and fragments in the renal tubular lumen. Inflammatory infiltration of the kidney induced apoptosis, which resulted in TECs loss that is characteristic of acute kidney diseases.<sup>51,52</sup> VX-702 treatment significantly reduced the number of TUNEL-positive cells. Taken together, these results indicated that VX-702 inhibited TECs apoptosis and the production of proinflammatory cytokines.

A critical question that remains unanswered is whether VX-702 directly inhibits p38 MAPK in TECs or via indirect inhibition involving other cell types. Guanwen Huang et al have proposed that LPS directly induces apoptosis of TECs.<sup>53</sup> Previous studies revealed that LPS enhanced the apoptosis of TECs at doses between 1 and 100  $\mu\text{g/mL}$ .<sup>32–35</sup> However, we found no difference in cell viability and apoptosis in TCMK-1 cells treated with different doses, compared to cells without LPS treatment. Therefore, we speculated that other cell types may be chiefly involved in S-AKI, instead of the LPS direct inhibition. Macrophages may play a vital role during inflammatory response, serving as the first line of defense against infections.<sup>54</sup> During the early stage of sepsis, macrophages secrete many proinflammatory factors and chemokines, which aggravate the inflammatory response.<sup>55,56</sup> However, excessive apoptosis of macrophages during late-stage sepsis results in immune dysfunction and organ injury.<sup>57</sup> In our study, we demonstrated that macrophages were directly involved in tubular epithelial cell apoptosis in S-AKI. In vivo, the numbers of F4/80<sup>+</sup> macrophages were increased in S-AKI group, the location of proinflammatory cytokines (IL-6 and IL-1 $\beta$ ) appeared to colocalize with F4/80<sup>+</sup> macrophages. In vitro, the viability of TCMK-1 cells co-cultured with LPS-induced RAW 264.7 cells was significantly decreased and the number of apoptotic cells was significantly increased compared to LPS-induced TCMK-1 cells. VX-702 inhibited apoptosis and enhanced the viability of TCMK-1 cells in the co-culture system. In contrast to the conventional view, our study provides evidence that LPS does not directly induce apoptosis of TECs.

We found that VX-702 treatment significantly suppressed LPS-induced expression of proinflammatory cytokines (IL-6, pro IL-1 $\beta$ , and cleaved IL-1 $\beta$ ) in macrophages. Furthermore, our data showed that VX-702 suppressed p38 MAPK phosphorylation in LPS-induced macrophages. These results suggested that the anti-inflammatory effects of VX-702 on S-AKI were associated with the inhibition of p38 MAPK phosphorylation. The protective mechanism of VX-702 in S-AKI may be that VX-702 treatment reduces the activity of p38 MAPK signaling pathway, resulting in decreased proinflammatory cytokines in macrophages, and hence mitigates the apoptosis of TECs. (Figure 9)

Molecular docking was performed to predict the binding energy of VX-702 with the hub genes. The binding energy of VX-702 with IL-6, IL-1 $\beta$ , and MAPK were all below zero. Then, we simulated the effect of VX-702 binding with cytokines (IL-6 and IL-1 $\beta$ ) and their receptors. The results showed that VX-702 induced a notable alteration in the molecular conformation of the IL-1 $\beta$  receptor and mildly increased the binding energy of IL-1 $\beta$  with its receptor,

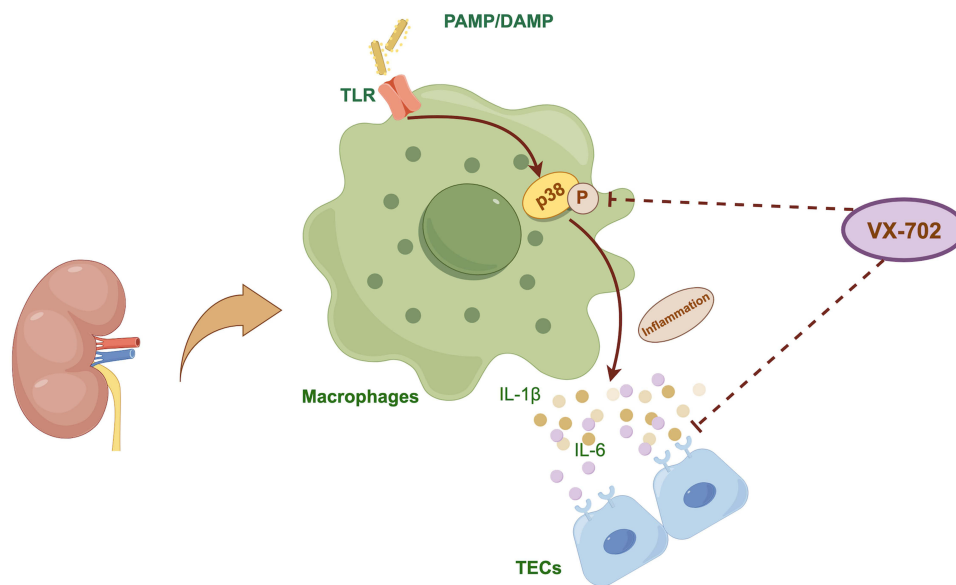


**Figure 9** The hypothesis of VX-702 alleviates the S-AKI.

**Abbreviations:** DAMP, damage-associated molecular patterns. PAMP, pathogen-associated molecular pattern. TECs, tubular epithelial cells. TLR, toll-like receptors. IL, interleukin.

suggesting that the binding of IL-1 $\beta$  and its receptor was weakened upon VX-702 treatment. This indicated that VX-702 might mitigate the severity of S-AKI by inhibiting the production of proinflammatory cytokines via the MAPK pathway and the binding of proinflammatory cytokines with their receptors simultaneously. (Figure 9)

This study provides new therapeutic strategies for S-AKI patients. Besides TECs, macrophages may be another therapeutic potential target and molecular marker for S-AKI. Early use of VX-702 may protect TECs from damage by inhibiting the release and binding of proinflammatory cytokines during sepsis, which could treat S-AKI patients before organic lesions. Whether VX-702 has a therapeutic effect on damaged TECs, and the feasibility of combining it with other drugs to treat S-AKI will need future experiments.

This study had certain limitations. First, although TECs and macrophages play vital roles in S-AKI, our high-throughput sequencing experiment included all types of cells in the kidney tissue. Hence, we need to analyze the specific gene expression of other cell types in the kidney. Second, single sample was used for the analysis of high-throughput sequencing, which may limit the ability to recapitulate the underlying genetic fully. Our further study on more kidney samples from mice and patients with S-AKI will be included. Third, the protective mechanism of VX-702 in S-AKI by blocking p38 MAPK Signaling was a supposition, which require further exploration and rescue treatment. Additionally, we predicted that VX-702 may bind IL-6 and IL-1 $\beta$  directly by molecular docking, which needs further experimental evidence.

## Conclusion

In conclusion, we demonstrated that VX-702 reduces tubular epithelial cell apoptosis and ameliorates S-AKI by inhibiting proinflammatory cytokines release in macrophages, which indicates its potential as a novel treatment for S-AKI.

## Abbreviations

AKI, acute kidney injury. BUN, blood urea nitrogen. CCK-8, cell counting kit-8. DAMPs, damage-associated molecular patterns. DAVID, Database for Annotation, Visualization and Integrated Discovery. DEGs, different expressed genes. DMEM, Dulbecco's modified eagle medium. DMSO, dimethylsulphoxide. ELISA, enzyme-linked Immunosorbent Assay. FBS, fetal bovine serum. GO, Gene Ontology. HE, hematoxylin and eosin. PAS, Periodic Acid-Schiff. IL, interleukin. KEGG, Kyoto Encyclopedia of Genes and Genomes. LB, Luria-Bertani. LPS, lipopolysaccharide. MAPK,

mitogen-activated protein kinase. *P. aeruginosa*, *Pseudomonas aeruginosa*. PAMPs, pathogen-associated molecular patterns. PPI, protein-protein interaction. p-p38, phosphorylation of p38. PVDF, polyvinylidene fluoride. RAW264.7, mouse leukemic monocyte/macrophage cell line. ROS, reactive oxygen species. S-AKI, sepsis-associated acute kidney injury. SCr, serum creatinine. SD, standard deviation. TCMK-1, mouse kidney tubular epithelial cell line. TECs, tubular epithelial cells. TLR, toll-like receptors. TNF- $\alpha$ , tumor necrosis factor- $\alpha$ . TUNEL, TdT-mediated dUTP nick end labeling.

## Ethics Approval

The present study was approved by the Ethics Animal Committee at Capital Medical University on the use of animals in research and education. The ethical code of animal experiments is AEEI-2022-087 and AEEI-2022-090.

## Acknowledgments

We thank Beijing Chaoyang Hospital and Capital Medical University for providing the experimental place and the related software used in this study. We thank Dr. Dong Wang for his excellent technical assistance. Figure 9 in the text was drawn by Figdraw. The volcano plot in Figure 2B was drawn by Bioladder. This article was edited by Elsevier Language Editing Services.

## Author Contributions

All authors made a significant contribution to the work reported, whether that is in the conception, study design, execution, acquisition of data, analysis and interpretation, or in all these areas; took part in drafting, revising or critically reviewing the article; have agreed on the journal to which the article has been submitted; and agree to be accountable for all aspects of the work.

## Funding

No funding was received to assist with the preparation of this manuscript.

## Disclosure

The authors report no conflicts of interest in this work.

## References

1. Vincent JL, Opal SM, Marshall JC, Tracey KJ. Sepsis definitions: time for change. *Lancet*. 2013;381(9868):774–775. doi:10.1016/S0140-6736(12)61815-7
2. Uchino S, Kellum JA, Bellomo R, et al. Acute renal failure in critically ill patients: a multinational, multicenter study. *JAMA*. 2005;294(7):813–818. doi:10.1001/jama.294.7.813
3. Wang F, Zhang G, Lu Z, et al. Antithrombin III/SerpinC1 insufficiency exacerbates renal ischemia/reperfusion injury. *Kidney Int*. 2015;88(4):796–803. doi:10.1038/ki.2015.176
4. Desanti De Oliveira B, Xu K, Shen TH, et al. Molecular nephrology: types of acute tubular injury. *Nat Rev Nephrol*. 2019;15(10):599–612. doi:10.1038/s41581-019-0184-x
5. Huen SC. Targeting protein translation to prevent septic kidney injury. *J Clin Invest*. 2019;129(1):60–62. doi:10.1172/JCI125432
6. Hou P, Jia P, Yang K, et al. An unconventional role of an ASB family protein in NF- $\kappa$ B activation and inflammatory response during microbial infection and colitis. *Proc Natl Acad Sci U S A*. 2021;118(3):456.
7. Komada T, Muruve DA. The role of inflammasomes in kidney disease. *Nat Rev Nephrol*. 2019;15(8):501–520. doi:10.1038/s41581-019-0158-z
8. Bang S, Donnelly CR, Luo X, et al. Activation of GPR37 in macrophages confers protection against infection-induced sepsis and pain-like behaviour in mice. *Nat Commun*. 2021;12(1):1704. doi:10.1038/s41467-021-21940-8
9. van der Poll T, van de Veerdonk FL, Scicluna BP, Netea MG. The immunopathology of sepsis and potential therapeutic targets. *Nat Rev Immunol*. 2017;17(7):407–420. doi:10.1038/nri.2017.36
10. Crayne CB, Albeituni S, Nichols KE, Cron RQ. The Immunology of Macrophage Activation Syndrome. *Front Immunol*. 2019;10:119. doi:10.3389/fimmu.2019.00119
11. Karakike E, Giamarellos-Bourboulis EJ. Macrophage Activation-Like Syndrome: a Distinct Entity Leading to Early Death in Sepsis. *Front Immunol*. 2019;10:55. doi:10.3389/fimmu.2019.00055
12. Damjanov N, Kauffman RS, Spencer-Green GT. Efficacy, pharmacodynamics, and safety of VX-702, a novel p38 MAPK inhibitor, in rheumatoid arthritis: results of two randomized, double-blind, placebo-controlled clinical studies. *Arthritis Rheum*. 2009;60(5):1232–1241. doi:10.1002/art.24485



13. Li Y, Zhou J. A Preliminary Exploration of the Efficacy of Gentamicin Sponges in the Prevention and Treatment of Wound Infections. *Infect Drug Resist.* 2021;14:2633–2644. doi:10.2147/idr.S315105
14. Zheng X, Zheng Y, Wang J, et al. Binimetinib ameliorates the severity of septic cardiomyopathy by downregulating inflammatory factors. *Int Immunopharmacol.* 2022;113(Pt B):109454. doi:10.1016/j.intimp.2022.109454
15. Wang D, Liu Y, Zhao Y, Zhou J. Low dose of protein A pretreatment can alleviate the inflammatory reaction and the bio-safety was evaluated in vivo. *J Chin Med Assoc.* 2016;79(7):400–408. doi:10.1016/j.jcma.2016.01.010
16. Wang X, Veeraraghavan J, Liu CC, et al. Therapeutic Targeting of Nemo-like Kinase in Primary and Acquired Endocrine-resistant Breast Cancer. *Clin Cancer Res.* 2021;27(9):2648–2662. doi:10.1158/1078-0432.Ccr-20-2961
17. Marasinghe CK, Jung WK, Je JY. Phloroglucinol possesses anti-inflammatory activities by regulating AMPK/Nrf2/HO-1 signaling pathway in LPS-stimulated RAW264.7 murine macrophages. *Immunopharmacol Immunotoxicol.* 2023;45(5):571–580. doi:10.1080/08923973.2023.2196602
18. Jang AY, Rod-In W, Monmai C, Choi GS, Park WJ. Anti-inflammatory effects of neutral lipids, glycolipids, phospholipids from Halocynthia aurantium tunic by suppressing the activation of NF- $\kappa$ B and MAPKs in LPS-stimulated RAW264.7 macrophages. *PLoS One.* 2022;17(8):e0270794. doi:10.1371/journal.pone.0270794
19. Faist A, Schloer S, Mecate-Zambrano A, et al. Inhibition of p38 signaling curtails the SARS-CoV-2 induced inflammatory response but retains the IFN-dependent antiviral defense of the lung epithelial barrier. *Antiviral Res.* 2023;209:105475. doi:10.1016/j.antiviral.2022.105475
20. Zhang D, Wang Y, Zeng S, et al. Integrated Analysis of Prognostic Genes Associated With Ischemia-Reperfusion Injury in Renal Transplantation. *Front Immunol.* 2021;12:747020. doi:10.3389/fimmu.2021.747020
21. Kinsey GR, Huang L, Jaworska K, et al. Autocrine adenosine signaling promotes regulatory T cell-mediated renal protection. *J Am Soc Nephrol.* 2012;23(9):1528–1537. doi:10.1681/asn.2012010070
22. Kinsey GR, Huang L, Vergis AL, Li L, Okusa MD. Regulatory T cells contribute to the protective effect of ischemic preconditioning in the kidney. *Kidney Int.* 2010;77(9):771–780. doi:10.1038/ki.2010.12
23. Sugawara H, Moniwa N, Kuno A, et al. Activation of the angiotensin II receptor promotes autophagy in renal proximal tubular cells and affords protection from ischemia/reperfusion injury. *J Pharmacol Sci.* 2021;145(2):187–197. doi:10.1016/j.jphs.2020.12.001
24. Szklarczyk D, Gable AL, Nastou KC, et al. The STRING database in 2021: customizable protein-protein networks, and functional characterization of user-uploaded gene/measurement sets. *Nucleic Acids Res.* 2021;49(D1):D605–d612. doi:10.1093/nar/gkaa1074
25. Szklarczyk D, Gable AL, Lyon D, et al. STRING v11: protein-protein association networks with increased coverage, supporting functional discovery in genome-wide experimental datasets. *Nucleic Acids Res.* 2019;47(D1):D607–d613. doi:10.1093/nar/gky1131
26. Shannon P, Markiel A, Ozier O, et al. Cytoscape: a software environment for integrated models of biomolecular interaction networks. *Genome Res.* 2003;13(11):2498–2504. doi:10.1101/gr.1239303
27. Otasek D, Morris JH, Bouças J, Pico AR, Demchak B. Cytoscape Automation: empowering workflow-based network analysis. *Genome Biol.* 2019;20(1):185. doi:10.1186/s13059-019-1758-4
28. Huang da W, Sherman BT, Lempicki RA. Systematic and integrative analysis of large gene lists using DAVID bioinformatics resources. *Nat Protoc.* 2009;4(1):44–57. doi:10.1038/nprot.2008.211
29. Huang da W, Sherman BT, Lempicki RA. Bioinformatics enrichment tools: paths toward the comprehensive functional analysis of large gene lists. *Nucleic Acids Res.* 2009;37(1):1–13. doi:10.1093/nar/gkn923
30. Sheikh-Hamad D, Cacini W, Buckley AR, et al. Cellular and molecular studies on cisplatin-induced apoptotic cell death in rat kidney. *Arch Toxicol.* 2004;78(3):147–155. doi:10.1007/s00204-003-0521-4
31. Solanki MH, Chatterjee PK, Gupta M, et al. Magnesium protects against cisplatin-induced acute kidney injury by regulating platinum accumulation. *Am J Physiol Renal Physiol.* 2014;307(4):F369–F384. doi:10.1152/ajprenal.00127.2014
32. Li J, Wang L, Wang B, et al. NOX4 is a potential therapeutic target in septic acute kidney injury by inhibiting mitochondrial dysfunction and inflammation. *Theranostics.* 2023;13(9):2863–2878. doi:10.7150/thno.81240
33. Tan C, Gu J, Li T, et al. Inhibition of aerobic glycolysis alleviates sepsis-induced acute kidney injury by promoting lactate/Sirtuin 3/AMPK-regulated autophagy. *Int J Mol Med.* 2021;47(3).
34. Xu L, Cai J, Li C, et al. 4-Octyl itaconate attenuates LPS-induced acute kidney injury by activating Nrf2 and inhibiting STAT3 signaling. *Mol Med.* 2023;29(1):58. doi:10.1186/s10020-023-00631-8
35. Zhang Y, Wang L, Meng L, Cao G, Wu Y. Sirtuin 6 overexpression relieves sepsis-induced acute kidney injury by promoting autophagy. *Cell Cycle.* 2019;18(4):425–436. doi:10.1080/15384101.2019.1568746
36. Bagshaw SM, Uchino S, Bellomo R, et al. Septic acute kidney injury in critically ill patients: clinical characteristics and outcomes. *Clin J Am Soc Nephrol.* 2007;2(3):431–439. doi:10.2215/CJN.03681106
37. Manrique-Caballero CL, Del Rio-Pertuz G, Gomez H. Sepsis-Associated Acute Kidney Injury. *Crit Care Clin.* 2021;37(2):279–301. doi:10.1016/j.ccc.2020.11.010
38. Cuenca AG, Delano MJ, Kelly-Scumpia KM, Moldawer LL, Efron PA. Cecal ligation and puncture. *Curr Protoc Immunol.* 2010. doi:10.1002/0471142735.im1913s91
39. Taveira da Silva AM, Kaulbach HC, Chuidian FS, Lambert DR, Suffredini AF, Danner RL. Brief report: shock and multiple-organ dysfunction after self-administration of Salmonella endotoxin. *N Engl J Med.* 1993;328(20):1457–1460. doi:10.1056/nejm199305203282005
40. Zhao Y, Wang ZY, Zhang XD, Wang Y, Yang WH, Xu YC. The Diagnostic Values of Peptidoglycan, Lipopolysaccharide, and (1,3)-Beta-D-Glucan in Patients with Suspected Bloodstream Infection: a Single Center, Prospective Study. *Diagnostics (Basel).* 2022;12(6).
41. Hotchkiss RS, Karl IE. The pathophysiology and treatment of sepsis. *N Engl J Med.* 2003;348(2):138–150. doi:10.1056/NEJMra021333
42. Fry DE. Sepsis, systemic inflammatory response, and multiple organ dysfunction: the mystery continues. *Am Surg.* 2012;78(1):1–8.
43. Kalakeche R, Hato T, Rhodes G, et al. Endotoxin uptake by S1 proximal tubular segment causes oxidative stress in the downstream S2 segment. *J Am Soc Nephrol.* 2011;22(8):1505–1516. doi:10.1681/ASN.2011020203
44. Schieven GL. The biology of p38 kinase: a central role in inflammation. *Curr Top Med Chem.* 2005;5(10):921–928. doi:10.2174/1568026054985902
45. Van Amersfoort ES, Van Berkel TJ, Kuiper J. Receptors, mediators, and mechanisms involved in bacterial sepsis and septic shock. *Clin Microbiol Rev.* 2003;16(3):379–414. doi:10.1128/cmr.16.3.379-414.2003

46. Kumar S, Boehm J, Lee JC. p38 MAP kinases: key signalling molecules as therapeutic targets for inflammatory diseases. *Nat Rev Drug Discov.* 2003;2(9):717–726. doi:10.1038/nrd1177
47. Saklatvala J. The p38 MAP kinase pathway as a therapeutic target in inflammatory disease. *Curr Opin Pharmacol.* 2004;4(4):372–377. doi:10.1016/j.coph.2004.03.009
48. Ma L, Zhao Y, Wang R, et al. 3,5,4'-Tri-O-acetylresveratrol Attenuates Lipopolysaccharide-Induced Acute Respiratory Distress Syndrome via MAPK/SIRT1 Pathway. *Mediators Inflamm.* 2015;2015:143074. doi:10.1155/2015/143074
49. Bode JG, Ehling C, Häussinger D. The macrophage response towards LPS and its control through the p38(MAPK)-STAT3 axis. *Cell Signal.* 2012;24(6):1185–1194. doi:10.1016/j.cellsig.2012.01.018
50. Cavender M, O'Donoghue M, Abbate A, et al. Inhibition of p38 MAP kinase in patients with ST-elevation myocardial infarction - findings from the LATITUDE-TIMI 60 trial. *Am Heart J.* 2022;243:147–157.
51. Peerapornratana S, Manrique-Caballero CL, Gómez H, Kellum JA. Acute kidney injury from sepsis: current concepts, epidemiology, pathophysiology, prevention and treatment. *Kidney Int.* 2019;96(5):1083–1099. doi:10.1016/j.kint.2019.05.026
52. Gao L, Wu WF, Dong L, et al. Protocatechuic Aldehyde Attenuates Cisplatin-Induced Acute Kidney Injury by Suppressing Nox-Mediated Oxidative Stress and Renal Inflammation. *Front Pharmacol.* 2016;7:479. doi:10.3389/fphar.2016.00479
53. Huang G, Bao J, Shao X, et al. Inhibiting pannexin-1 alleviates sepsis-induced acute kidney injury via decreasing NLRP3 inflammasome activation and cell apoptosis. *Life Sci.* 2020;254:117791. doi:10.1016/j.lfs.2020.117791
54. Huang X, Xiu H, Zhang S, Zhang G. The Role of Macrophages in the Pathogenesis of ALI/ARDS. *Mediators Inflamm.* 2018;2018:1264913. doi:10.1155/2018/1264913
55. Lauvau G, Loke P, Hohl TM. Monocyte-mediated defense against bacteria, fungi, and parasites. *Semin Immunol.* 2015;27(6):397–409. doi:10.1016/j.smim.2016.03.014
56. Hamidzadeh K, Christensen SM, Dalby E, Chandrasekaran P, Mosser DM. Macrophages and the Recovery from Acute and Chronic Inflammation. *Annu Rev Physiol.* 2017;79:567–592. doi:10.1146/annurev-physiol-022516-034348
57. Wang TS, Deng JC. Molecular and cellular aspects of sepsis-induced immunosuppression. *J Mol Med (Berl).* 2008;86(5):495–506. doi:10.1007/s00109-007-0300-4

Journal of Inflammation Research

Dovepress

## Publish your work in this journal

The Journal of Inflammation Research is an international, peer-reviewed open-access journal that welcomes laboratory and clinical findings on the molecular basis, cell biology and pharmacology of inflammation including original research, reviews, symposium reports, hypothesis formation and commentaries on: acute/chronic inflammation; mediators of inflammation; cellular processes; molecular mechanisms; pharmacology and novel anti-inflammatory drugs; clinical conditions involving inflammation. The manuscript management system is completely online and includes a very quick and fair peer-review system. Visit <http://www.dovepress.com/testimonials.php> to read real quotes from published authors.

Submit your manuscript here: <https://www.dovepress.com/journal-of-inflammation-research-journal>